

A Simple and Convenient Set-Up of Light Addressable Potentiometric Sensors (LAPS) for Chemical Imaging Using a Commercially Available Projector as a Light Source

Yen-Heng Lin^{1,2,3,*}, Anirban Das¹, and Chao-Sung Lai^{1,2,*}

¹Department of Electronic Engineering, Chang Gung University, Taoyuan, Taiwan 333

²Healthy Aging Research Center, Chang Gung University, Taoyuan 333, Taiwan

³Graduate Institute of Medical Mechatronics, Chang Gung University, Taoyuan 333, Taiwan

*E-mail: yenheng@mail.cgu.edu.tw; cslai@mail.cgu.edu.tw

Received: 8 March 2013 / Accepted: 28 March 2013 / Published: 1 May 2013

Light addressable potentiometric sensors (LAPS) are important semiconductor based label free sensing tools that are useful for visualizing the 2-D distribution of chemical species because of their light addressing capability at measurement sites. However, the expense and complexity of the LAPS light modulation set-up is highly inconvenient. To address this issue, we demonstrate a simple and convenient LAPS set-up that uses a commercially available projector as a programmable scanning light source. In the proposed set-up, an illuminated light spot used to excite electron-hole pairs in silicon was generated from a projector and an objective lens with the aid of commercially available computer software. Using a projector is an easy and flexible method of controlling the shape, size, movement, and the modulation frequency of the measurement spot in a user defined manner through a computer software interface. This approach avoids the complexity associated with using an X-Y stage or multiple light sources for scanning the LAPS surface. In addition, it reduces the setup time for the optical system and language programming for the control of digital micro-mirror device by using ARM-based processor. Using the set-up developed here, a minimum measurement spot of size 22x22 μm^2 was achieved. Additionally, the photoresponse-voltage characteristics, constant bias measurement and the pH sensitivity were successfully studied with this set-up. Finally, the pH imaging ability of this setup was successfully demonstrated.

Keywords: Light-addressable-potentiometric-sensor (LAPS), projector, chemical imaging, solid-state sensor

1. INTRODUCTION

Recently, there has been a great deal of research in semiconductor based biosensors due to their immense potential for label free detection, as well as the ease of integration with miniaturized systems.

There are three basic types of semiconductor based field-effect chemical sensors: (i) ion sensitive field-effect transistors (ISFET) [1,2], (ii) electrolyte-insulator-semiconductor (EIS) capacitance based sensors [3], and (iii) light addressable potentiometric sensors (LAPS) [4–6]. Among them, LAPS was first introduced by Hafeman *et al.* in 1988 [4] by combining the scanned light pulse technique (SLPT) [7] with an EIS sensor. As a consequence, a LAPS is very similar in structure to an EIS capacitive sensor. The major difference between LAPS and EIS sensors is that in LAPS the change of capacitance of the depletion layer at the insulator and semiconductor surface is detected by measuring the local photocurrent generated at the point of illumination. A DC voltage is applied to the LAPS structure, which has an ionic group on the electrolyte-insulator surface, so that the depletion layer develops at the insulator-semiconductor interface. When the modulated light, or local stimulus, illuminates the semiconductor substrate, electron-hole pairs are generated in the substrate. Additionally, an AC photocurrent is induced as a consequence of the electron hole pair separation in the electric field in depletion layer. The amplitude of this photocurrent is influenced by the width of the depletion layer at the illuminated point. However, the width of the depletion layer depends on the local Nernstian potential at the analyte/transducer interface. Therefore, by monitoring the AC photocurrent of LAPS, any change in the analyte concentration can be obtained spatially [8–11]. The working principle of LAPS gives it the unique ability to address individual sensing sites by utilizing a modulated light beam. The concept of addressing a measurement site allows this relatively simple structure the ability to sense the bio-chemical processes on a chip surface spatially without any complex bonding, wiring or encapsulation. For example, LAPS have been employed successfully to biological applications such as immunoassays [12,13], drug analysis [14,15], cell metabolism [16], and extracellular measurements [17].

In addition to these advantages, the light addressing ability of LAPS makes it a valuable tool for visualizing two-dimensional distributions of chemical species' concentrations by scanning and measuring the corresponding photosignal at the sensing surface. The photosignal at each measurement spot can be mapped into a color representation and utilized as a "pixel" to generate a chemical image of the electrochemical properties at the LAPS surface. Chemical image sensors have wide applications in various fields of biology and chemistry. For example, LAPS based imaging technique have been successfully adapted to visualize the biological activity of biological systems such as *Escherichia coli* [18] and enzymes [19], as well as to monitor the ionic diffusion in electrochemical systems [20] and multi ion imaging [21].

The light addressing technique in LAPS set-up is an important issue in the sense of the flexibility, miniaturization and speed of the measurement system. There are two basic approaches of addressing the measurement spot in a pixel-by-pixel manner on the sensing surface in a LAPS set-up. The conventional approach utilizes a mechanical X-Y stage and a focused laser beam to address the measurement spot one pixel at time on the LAPS surface [22,23]. Although this method offers high resolution sensing, the laser beam is a large in size and highly expensive, and the positioning stage has size and speed limitations. In another approach, multiple light sources are illuminated simultaneously using different modulation frequencies. The received signal is the sum of the signals at each of the frequency components. The individual frequency components, which correspond to different measurement sites, can then be extracted individually using a fast Fourier transformation (FFT)

algorithm [24]. Although this approach significantly reduces the measurement time, it has the drawback of having a limited number of light sources. Additionally, the size and shape of the light spot cannot be controlled in an optimal manner during the measurement time of the above-mentioned scanning procedure. Recently, digital light processing (DLP) technology was employed as the scanning light source in a LAPS set-up in order to generate a chemical image with an arbitrarily shaped and sized light spot [25]. However, in this method, an ARM-based processor board was used to access the internal digital micro-mirror device (DMD) control, which requires extensive development time and ability. Additionally, the setup of this optical system requires sophisticated optical techniques and components, which is an additional barrier to implementation.

In this study, a simple and convenient approach that utilizes a commercially available projector in combination with an objective lens as a programmable scanning light source for a LAPS set-up was proposed. The modulated light spots used in this set-up were drawn on personal computer (PC) with commercially available software (Microsoft Powerpoint or Adobe Flash) and then projected from a projector through a microscope objective. The size, shape, and frequency of the light spot can be modified simply by computer aided control. By using this setup for scanning, there was no need to mechanically move the light source. This simple set-up has also successfully provided a straightforward method for flexible chemical imaging.

2. EXPERIMENTAL PART

2.1. Set-up of projector based LAPS platform

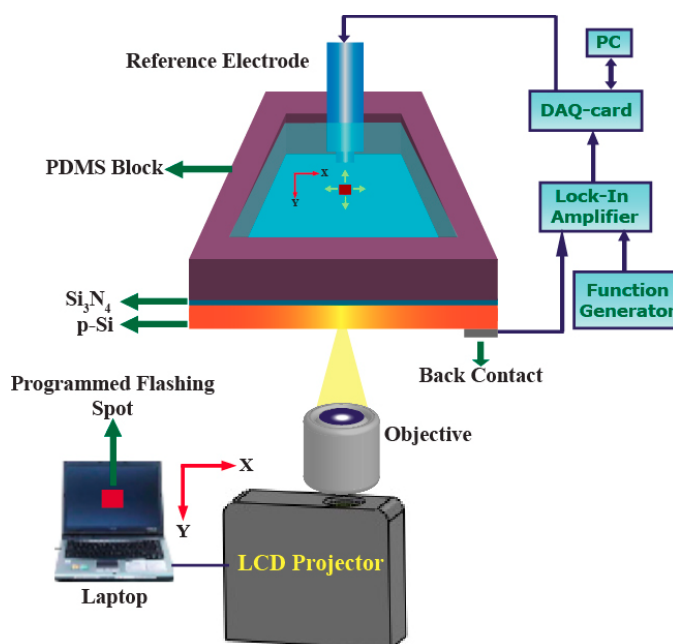


Figure 1. Schematic illustration of a projector based LAPS set-up. The shape, size, and flashing frequency of the image can be programmed by a computer and the image can be projected from a commercial projector through an objective lens.

The schematic illustration of the experimental set-up of the projector based LAPS measurement system is depicted in fig. 1. A liquid crystal based, commercially available projector (PLC-XU350, Sanyo, Japan) is used as the excitation light source in this set-up and placed underneath the LAPS chip. The light beam diverging from the projector is focused on the LAPS chip by placing a 50x objective lens (ELWD 50X, Nikon, Japan) in between the projector and the chip. In this set-up, the projector serves as an optical source, and also allows the system to take advantage of the convenience of control by a personal computer (PC) user interface. The measurement spots can be defined by drawing images on a PC using commercially available software (Adobe Flash). The position, size, shape, movement, and modulation frequency of the light spot are defined by programming the images via the PC interface. Finally, the image from the projector is collected and collimated onto the LAPS chip by using the objective lens. The focusing system generates a circular measurement window with a diameter of 1.35 mm on the LAPS chip. The size of the measurement area can be determined from the magnification of the lens. However, when a lower lens magnification is used to generate a larger measurement area, the size of light spot increases, and thus, the spatial resolution of the measurement decreases. This simple projector based optical set-up allows the LAPS measurement technique to provide enormous versatility while at the same time removing the complexity of using an X-Y stage or multiple light sources. The measured photocurrent from the chip is converted to voltage and amplified by a lock-in amplifier (SR510, Stanford Research Systems Inc., California, USA). A function generator (33210A, Agilent, USA) is employed as the source of the reference signal, which has the same modulation frequency as the light spot from the projector. This signal is fed into the reference input of the lock-in-amplifier. The amplified signal is then sampled and recorded with a 16-bit data acquisition card (PCI 6221, National Instrument, USA) by a LabView based program on PC. The program is also used to generate a bias voltage sweep and constant voltage through the DAQ card to an Ag/AgCl reference electrode. The waveform nature of the generated photocurrent is amplified by using a variable gain low noise preamplifier (DLPCA 200, FEMTO, Berlin, Germany). Chemical imaging of different pH buffers was achieved by storing the photoresponse data at each different scanning position during the constant reference voltage measurement. The stored data were then converted into color map in a pixel wise manner.

2.2. Fabrication process of LAPS chip

For the LAPS chip fabrication, a 4 inch p-type (<100>, resistivity: 5-10 Ω -cm) silicon (Si) wafer was used for the substrate. A 60 nm thick Si_3N_4 layer was then deposited by a low pressure chemical vapor deposition (LPCVD) system for use as a sensing membrane. Next, the backside Si_3N_4 was removed by a reactive ion etching (RIE) process in a CF_4 (40 sccm) and O_2 (20 sccm) mixture ambient under a processing pressure of 100 mT and an RF power of 100 W. After that, a 300 nm thick Aluminum (Al) layer was deposited onto the backside of the Si wafer for ohmic contact by thermal evaporation. To open an illumination area on the backside of the chip, a part of the Al layer was patterned by photo-lithography and removed with an Al etchant. The wafer was then cut into pieces and attached on a copper line of printed circuit board (PCB) that had an open window for the

illumination. Finally, a Polydimethylsiloxane (PDMS) structure was used as a buffer solution container. After the master mold was fabricated, the silicone elastomer and the elastomer curing agent, PDMS, (Sylgard 184A and 184B, Sil-More Industrial Ltd., USA) were mixed in a 10:1 ratio and then poured onto the mold. After the degassing process, the mixture was cured at a temperature of 100°C for at least 2 hours. The inverse structures of the master mold were then transferred onto the PDMS. The PDMS container and the LAPS sensing substrate were then bonded together using an oxygen plasma treatment to form the LAPS chip. The sensing process described in this paper is accomplished by depositing the analyte onto this LAPS chip. All of the chemical reagents, including the pH level solution, were purchased from Sigma-Aldrich.

3. RESULTS AND DISCUSSION

3.1. Optimization modulation frequency of light source

In the present set-up, a liquid crystal display based commercial projector was utilized as a programmable light source to address the measurement spot on the LAPS chip. In such a set-up, no chopper was needed for the modulation of the light source because the modulation was programmed in adobe flash software. Programming the light spot involved making one frame with a white square on a black screen, the next frame with a completely black screen, and then repeating the first frame again. Then, these frames are rapidly displayed through the projector, the first frame will allow the square light spot to be projected, the second frame will block the light, and the next one will again allow the light. The rapid switching of the light between on and off produces a modulated light spot. The modulation frequency can be adjusted in a user defined manner by defining the frame rate in software. As a consequence, the modulation frequency becomes half of the frame rate set in the adobe flash software.

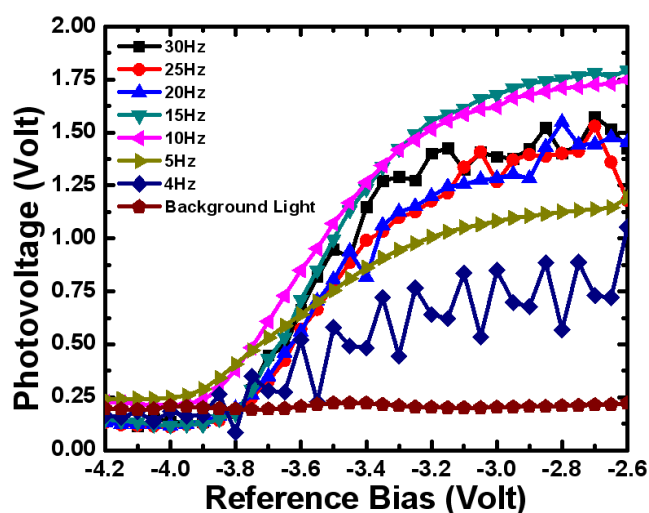


Figure 2. Photovoltage vs. reference bias plots for different modulation frequencies of the flashing spot defined by a projector based LAPS set-up. In the present set-up, the projector achieves the highest stable frequency of 15 Hz.

For example, a modulation frequency of 10 Hz will be created when the frame rate is set to 20 frame per second (fps). Additionally, the lateral movement of the spot can also be programmed simultaneously by moving the location of the white spot in the alternate frames. Finally, this programmed spot was projected through the objective onto the backside of the LAPS chip. To figure out the modulation capability of the present set-up, we measured the photovoltage of the LAPS chip at different modulation frequencies of the light spot. The corresponding photovoltage vs reference bias characteristic is shown in fig. 2. It shows that the best response is achieved at frequency of 15 Hz, which corresponds to a frame rate of 30 fps. For frame rates higher than 30 fps, the photovoltage vs reference bias characteristic of the LAPS chip began to deform. The maximum refresh rate of the projector is 100 Hz and the frame rate of the software can be set to 120 fps, which were higher than the 30 fps needed to achieve 15 Hz modulation. The maximum frequency of 15 Hz in this set-up may be due to the limitation of the software-hardware interface. On the other hand, for the frequencies lower than 15 Hz, the noise to the signal ratio increases with decreasing frequency. In general, the LAPS should be used with the modulation frequency which generates the highest signal-to-noise ratio [26,27] (typical at a frequency of 1 kHz). Such a high frequency cannot be achieved with this present set-up. However, experimental data shows a nearly sinusoidal wave response was obtained with the present set-up at frequencies as low as 15 Hz, as shown in fig. 3.

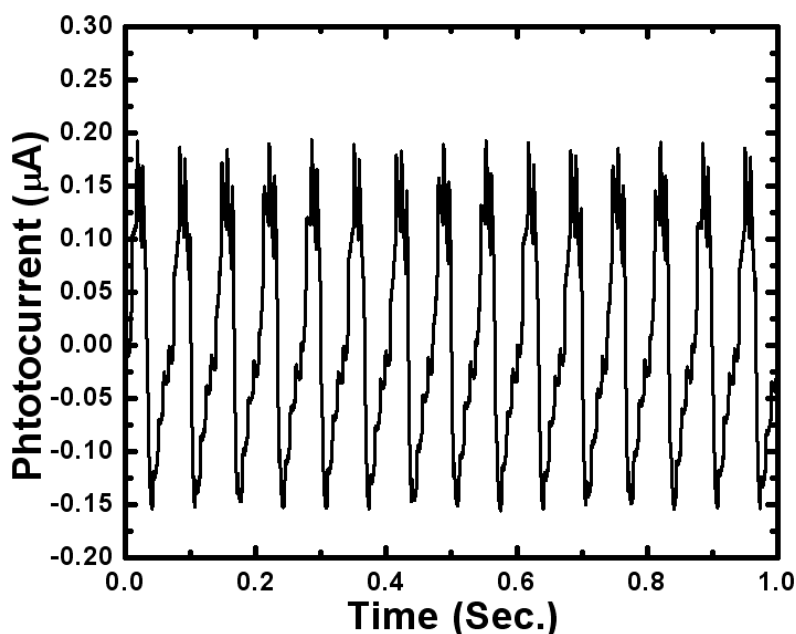


Figure 3. Photocurrent waveform of the LAPS chip generated by the light spot with a modulation frequency of 15 Hz.

These data reveal that it is possible to measure the corresponding photovoltage with trading high signal intensity for the ability to use low frequencies. The intensity of the measured photovoltage is sufficient to the chemical imaging application. As such, the optimum modulation frequency of 15 Hz is applied to all other experiment in this study.

3.2. Sensing result of pH level

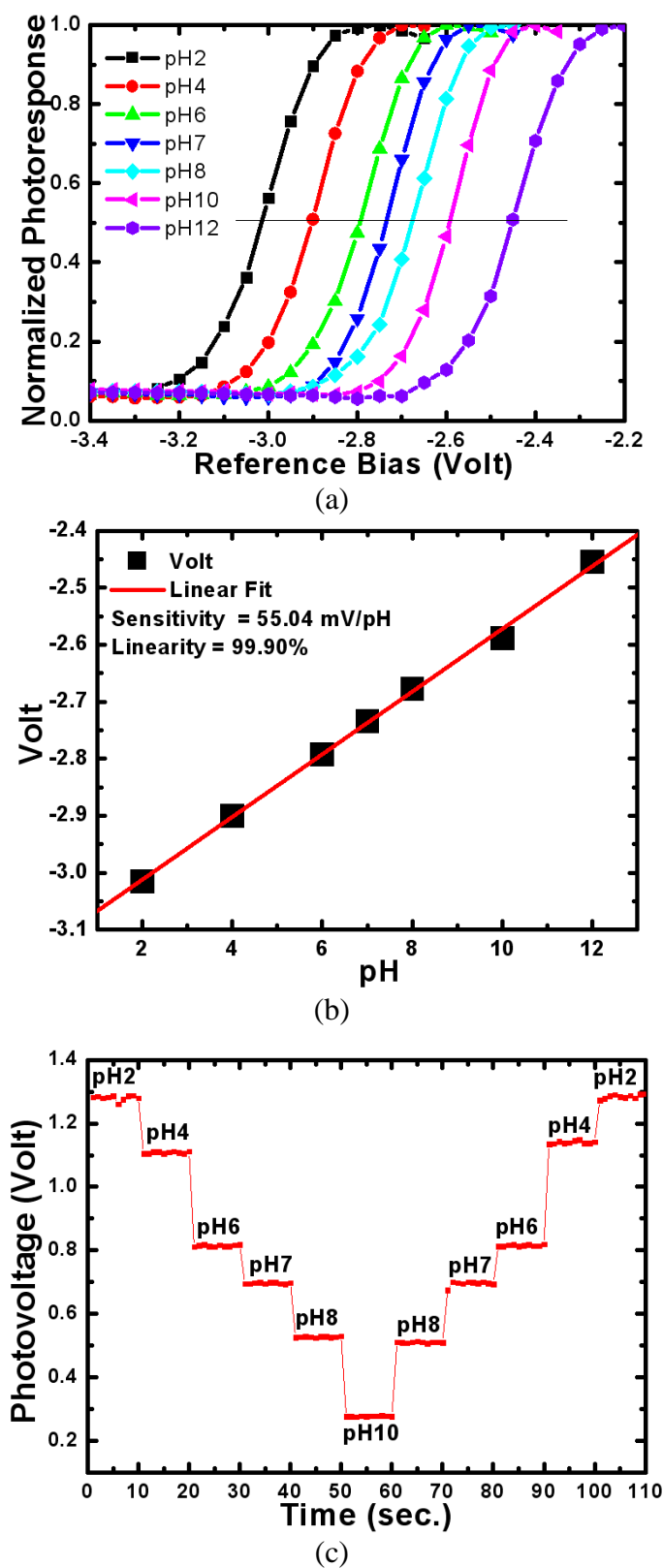


Figure 4. (a) Normalized photoresponse vs. reference bias characteristic of the LAPS chip for different pH buffers with a light spot size of $50 \times 50 \mu\text{m}^2$. (b) Sensitivity and linearity of the LAPS chip for measurement of pH values ranging from 2 to 12. (c) Constant bias measurement of the LAPS chip for different pH values.

To test the pH sensing performance of LAPS chip with the present set-up, a square shaped white spot of size $50 \times 50 \mu\text{m}^2$ was used to illuminate the LAPS chip. The amplitude of the photoresponse was measured as a function of the bias voltage for buffer solutions with different pH values. The corresponding measurement plot is depicted in fig. 4(a), which shows the shift of the photoresponse vs bias curve along the voltage axis as the pH value changes. According to the site-binding model [28], a potential difference appears at the interface of the sensing membrane (Si_3N_4) and the solution that depends on the concentration of H^+ in the electrolyte. The larger concentration of H^+ in solution leads to a larger potential difference, resulting in a shift of the photoresponse vs bias curve towards the negative side of the bias axis as the pH value decreases. To calculate the sensitivity and the linearity, the curve shift was plotted against the pH value as shown in fig. 4(b). The sensitivity of the measurement can be estimated by using following equation:

$$\text{Sensitivity} = \Delta V/\text{pH} \quad (1)$$

where ΔV is the change in the reference bias due to a change in pH at a constant photovoltage. The calculated sensitivity is approximately 55 mV/pH and has a linearity of 99.9%, which is in good agreement with the ideal Nernstian value. For the further application of constructing a chemical image, the result of the constant bias measurement mode becomes highly relevant. This mode is the fastest and suitable for chemical imaging because chemical imaging requires measuring the photosignal for a large numbers of pixels. Fig. 4(c) shows the measurement result of the constant bias mode. The amplitude change of the photosignal is plotted when the pH value of the buffer solution is varied from 2 to 10. Because of the limitation of the constant bias measurement, the photosignal shift between the pH values of 2-4 is smaller than the shifts between other pH value ranges [29]. In this case, the shift of photoresponse due to pH change (pH2 to pH4) reaches near to its saturation limit and results in the constraint of the photosignal shift.

3.3. Spot size and spatial resolution

The illumination spot size is one of the most important factors for determining the spatial resolution of LAPS [30]. It is believed that a smaller spot size allows higher resolution, and thus, more information about the chip surface that can be measured. To investigate the response of the chip as the spot size is varied; the photovoltage vs reference bias characteristic was measured for different sizes of square-shaped measurement spots. During this measurement, the software was programmed to change the spot size automatically after a certain interval of time. The LAPS chip was in contact with buffer solution of pH 2. It was observed that the amplitude of the photosignal decreased with decreasing measurement spot size. As the spot size decreases, fewer electron hole pairs are generated in the bulk Si and, therefore, fewer diffuse into the depletion region, which in turn results in a smaller photosignal. Experimental data depicted in fig. 5(a) shows that an acceptable photoresponse can be achieved with a total measurement spot area as small as $22 \times 22 \mu\text{m}^2$. The corresponding constant bias measurement at -3.183 volts is illustrated in fig. 5(b). The corresponding measured of the photosignal characteristic for

a measurement spot size of $22 \times 22 \mu\text{m}^2$ is shown in the inset of fig. 5(b). The photosignal for the $22 \times 22 \mu\text{m}^2$ spot was defined as $V_{\text{signal}} = V_{\text{spot}} - V_{\text{background}}$ and the corresponding fluctuation in the amplitude of the photovoltage was determined from the plot as ΔV_{noise} .

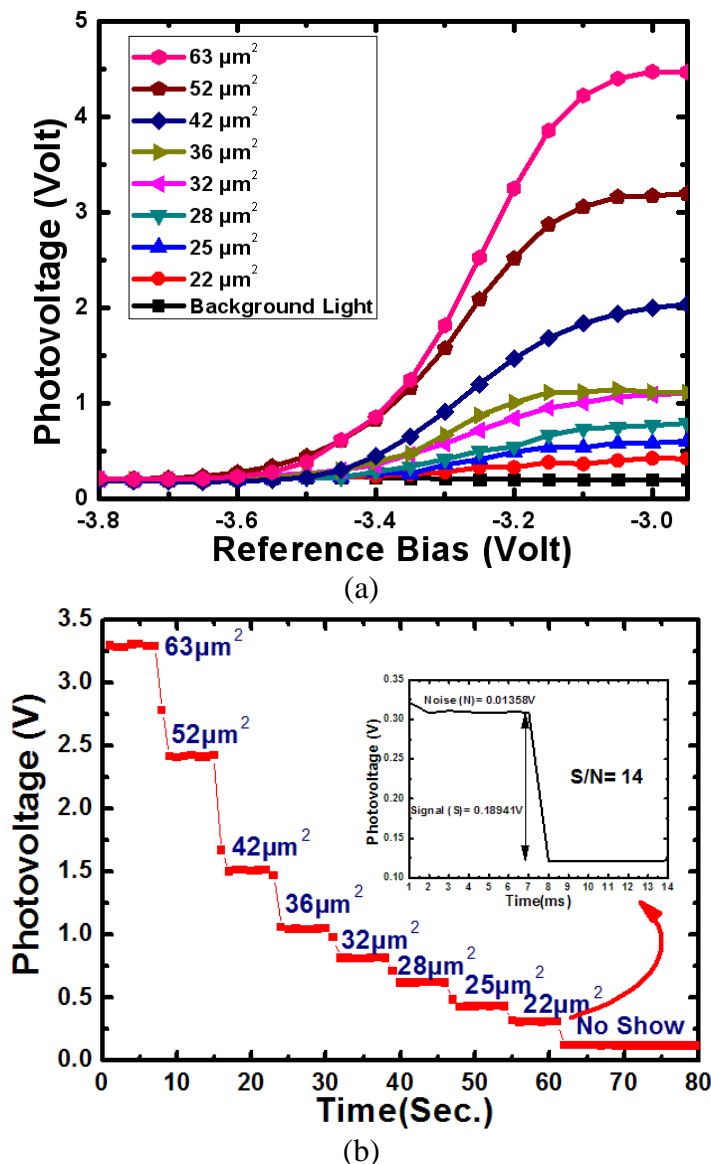


Figure 5. (a) Photovoltage vs. reference bias curves at pH2 for different sizes of the square shaped flashing spot of frequency 15 Hz generated by the new set-up. (b) Photoresponse of the LAPS chip at constant bias -3.183 volt for square shaped measurement spots that were programmed to decrease in size with time. The minimum spot size of $22 \times 22 \mu\text{m}^2$ is achieved with acceptable S/N value of approximately 14.

The normalization of the signal V_{spot} to the noise ΔV_{noise} led to a signal/noise (S/N) ratio of 14, which is reasonable. This S/N ratio for the minimum spot size of the present set-up is sufficient for use as the scanning source in conventional LAPS. Moreover, the projector used in this set-up provides contrast ratio as 500:1. It is expected that a projector with a higher contrast ratio and intensity would

allow for an even smaller spot size. Additionally, it is advantageous to use a higher resolution LAPS structure like GaAs, amorphous Si or thinner crystalline Si based LAPS.

3.4 Chemical imaging of pH buffer solution

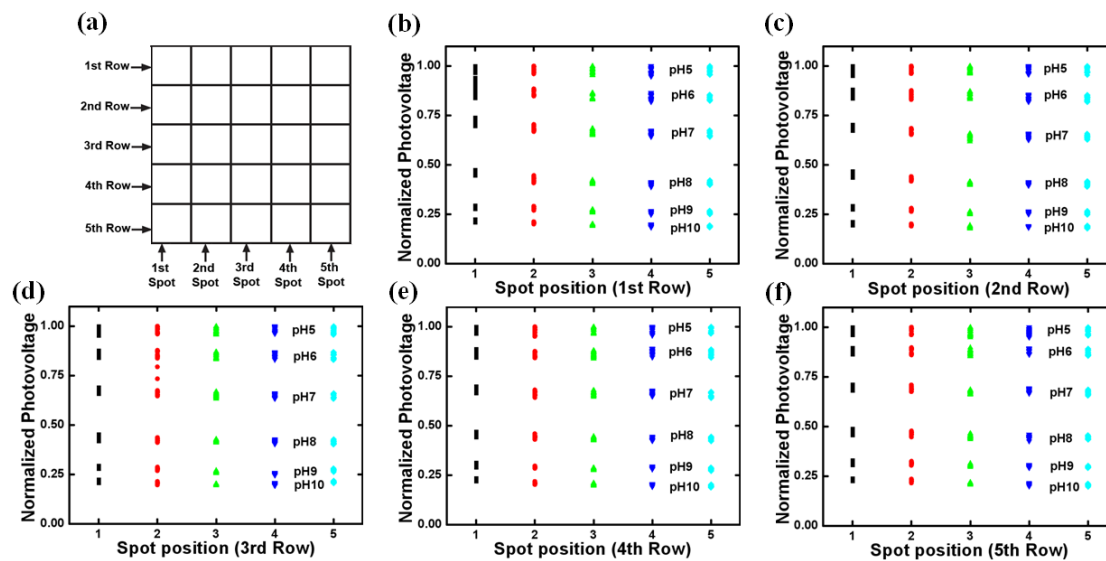


Figure 6. (a) Schematic illustration of the sensing area of the chemical imaging. (b)~(f) Normalized photoresponse at each point with different pH level from row 1 to row 5.

Chemical imaging of pH buffer solution has been successfully demonstrated using different scanning method in LAPS system [25, 31-34]. In this study, commercial video projector was used as a light addressing technique, which delivered a compact, simplified and user-friendly light-addressing tool by taking advantage of PC interface facility. To investigate the imaging capability of the present set up, a 5X5 array of measurement spots was programmed as shown in fig. 6(a). Each spot of this array was square shaped and had a dimension of $50 \times 50 \mu\text{m}^2$. The total scan area was $250 \times 250 \mu\text{m}^2$. In this set-up, a 50X objective lens was used to collect and collimate the programmed spots on the LAPS chip. As a result, the light intensity distribution across the scanning window was found to have a Gaussian profile. The intensity of the resulting spot was highest in the middle of the window, and declined as the spot was moved away from the center. For this reason, the scan area was restricted at the center region of the window. While using an objective lens with lower magnification increases the scan area, it also sacrifices the higher resolution that would be achieved with a smaller spot size. Changing the objective lens can be utilized as a “zoom-in” technique. Using an objective lens with a lower magnification will scan a larger area of the chip surface. A higher magnification objective lens can then be used to scan an interesting area with higher resolution. Despite the fact that the scanned area is confined to the center of projected area, a small variation of the photoresponse for the same pH was still observed due to the light intensity distribution. The trends in the distribution of the photovoltage for the six pH solutions were similar for each of the scanning rows. As expected, the light intensity distribution was the same for all pH buffers inside the sensing window. Additionally, we

attempted cancel the variation caused by the distribution of illuminating light by normalizing the photoresponse value. First, the photoresponse at each spot position (5X5) for pH values from 5 to 10 were recorded under a fixed bias voltage with 20 data points collected at each position. The total scanning time was 50 s to acquire (5X5)X20 data points for each pH level. The normalization process was performed on a row by row basis. Figure 6(b) shows the normalized photovoltages at the first row with 5 positions at different pH values. At the five positions of first row, the maximum values of photovoltage were found when measuring the pH 5 solution at each position. Then, all of the photovoltage values with different pH levels at the same position were divided by the maximum value at that position and then normalization was performed on the first row. The same normalization process was applied on the second to fifth row accordingly as shown in fig. 6(c)–(f).

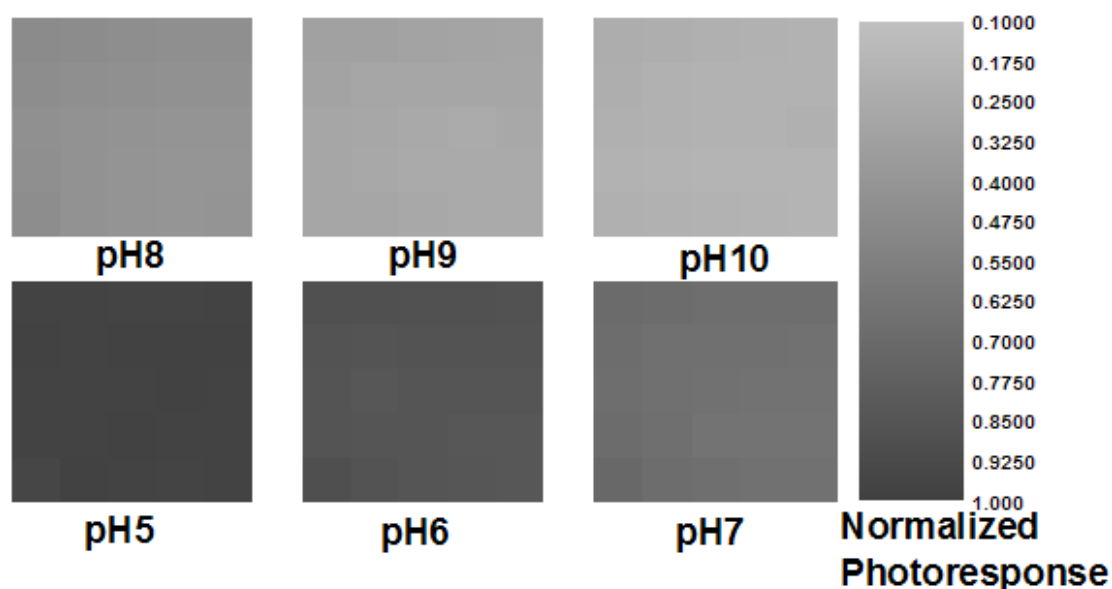


Figure 7. Chemical images of the different pH buffer solutions obtained by the projector based scanning system.

To verify the repeatability of measurements at the same position, the coefficient of variation (CV) between the twenty normalized values was calculated. From the comparison of 150 CVs from 25 positions at 6 pH levels, the maximum CV value was found to be 6.67% (at pH 6, row 3 and position 2). The variation may be caused by the control of the liquid crystal in projector, which may produce small variations in light intensity of the projector. For chemical imaging, the average of the twenty normalized values at each location was calculated and then converted into a color scale for display as a pixel. For each pH level, 25 pixels were mapped to form a pH level distribution image as shown in fig. 7. Lighter colors of the gray scale represent higher pH levels at the LAPS surface. The measuring uniformity of the entire measurement area for each pH value was evaluated by calculating the CV of the average value for the 25 positions. The maximum CV was calculated to be 6.77% at the pH level of 9, which is very close to the CV value calculated at a single position. This demonstrates a high measuring uniformity over the entire sensing area when the proper normalization process is performed.

The proposed set-up provides a promising tool for LAPS measurements and chemical imaging that is both cost-efficient and user-friendly.

4. CONCLUSIONS

In this work, a simple and convenient set-up of LAPS was developed, in which a commercially available projector was used as a programmable scanning light source to provide an uncomplicated method for flexible chemical imaging. Additionally, the need for mechanical movement of the light source was eliminated. The size, shape, movement and the modulation frequency were simply achieved by using a PC interface. The use of a projector in this set-up removed the need for the complicated optical and mechanical systems usually required in conventional LAPS measurement systems and miniaturized the set-up.

Currently, this set-up delivered a minimum measurement spot size of $22 \times 22 \mu\text{m}^2$ at a modulation frequency of 15 Hz. Both the pH sensitivity of the LAPS chip through a photovoltage vs bias characteristic and a constant bias measurement were achieved successfully. The programmed light spot was used to scan the LAPS surface and allowed chemical imaging to be performed in a straightforward manner. The results reveal that this commercially available projector based set-up has great potential to deliver an easy, flexible, and low cost programmable platform for LAPS measurements. This set-up provides a promising solution to the need for a simple chemical imaging system that can visualize the 2-D distribution of chemical species.

ACKNOWLEDGEMENTS

This work was sponsored by the National Science Council of Taiwan, Republic of China (100-2221-E-182-021-MY3)

References

1. P. Bergveld, *IEEE Trans. Biomed. Eng.*, BME-17 (1970) 70
2. T. Matsuo and K.D. Wise, *IEEE Trans. Biomed. Eng.*, BME 21 (1974) 485
3. L. Bousse, N.F. de Rooij and P. Bergveld, *IEEE Trans. Electron Devices*, 30 (1983) 1263
4. D.G. Hafeman, J.W. Parce and H.M. McConnell, *Science*, 240 (1988) 1182
5. J.C. Owicki, L. Bousse, D. Hafeman, G.L. Kirk, J.D. Olson, H.G. Wada and J.W. Parce, *Annu. Rev. Biophys. Biomol. Struct.*, 23 (1994) 87
6. T. Wagner and M.J. Schöning, *Electrochemical sensor analysis*, Elsevier, Amsterdam, Netherlands (2007).
7. O. Engström and A. Carlsson, *J. Appl. Phys.*, 54 (1983) 5245
8. M. Sartore, M. Adami and C. Nicolini, *Biosens. Bioelectron.*, 7 (1992) 57
9. M. Sartore, M. Adami, C. Nicolini, L. Bousse, S. Mostarshed and D. Hafeman, *Sens. Actuators A-Phys.*, 32 (1992) 431
10. W.J. Parak, U.G. Hofmann, H.E. Gaub and J.C. Owicki, *Sens. Actuators A-Phys.*, 63 (1997) 47
11. Q. Zhang, *Sens. Actuators B-Chem.*, 105 (2005) 304
12. W.E. Lee, H.G. Thompson, J.G. Hall and D.E. Bader, *Biosens. Bioelectron.*, 14 (2000) 795
13. H.G. Thompson and W.E. Lee, *Defence Research Establishment Suffield, Suffield Report*, 554

- (1991).
14. Y. Wu, P. Wang, X. Ye, Q. Zhang, R. Li, W. Yan and X. Zheng, *Biosens. Bioelectron.*, 16 (2001) 277
 15. Q. Liu, H. Yu, Z. Tan, H. Cai, W. Ye, M. Zhang and P. Wang, *Sens. Actuators B–Chem.*, 155 (2011) 214
 16. B. Stein, M. George, H.E. Gaub, J.C. Behrends and W.J. Parak, *Biosens. Bioelectron.*, 18 (2003) 31
 17. B. Stein, M. George, H.E. Gaub and W.J. Parak, *Sens. Actuators B–Chem.*, 98 (2004) 299
 18. T. Yoshinobu, H. Iwasaki, M. Nakao, S. Nomura, T. Nakanishi, S. Takamatsu and K. Tomita, *Bioimages*, 5 (1997) 143
 19. S. Inoue, M. Nakao, T. Yoshinobu and H. Iwasaki, *Sens. Actuators B–Chem.*, 32 (1996) 23
 20. T. Yoshinobu, T. Harada and H. Iwasaki, *Jpn. J. Appl. Phys.*, 39 (2000) L318.
 21. T. Yoshinobu, H. Iwasaki, Y. Ui, K. Furuichi, Y. Ermolenko, Y. Mourzina, T. Wagner, N. Näther and M.J. Schöning, *Methods*, 37 (2005) 94
 22. M. Nakao, S. Inoue, T. Yoshinobu and H. Iwasaki, *Sens. Actuators B–Chem.*, 34 (1996) 234
 23. T. Yoshinobu, N. Oba, H. Tanaka and H. Iwasaki, *Sens. Actuators A–Phys.*, 51 (1996) 231
 24. Z. Qintao, W. Ping, W.J. Parak, M. George and G. Zhang, *Sens. Actuators B–Chem.*, 73 (2001) 152
 25. T. Wagner, C.F. Werner, K.-i. Miyamoto, M.J. Schöning and T. Yoshinobu, *Sens. Actuators B–Chem.*, 170 (2012) 34
 26. L. Bousse, S. Mostarshed, D. Hafeman, M. Sartore, M. Adami and C. Nicolini, *J. Appl. Phys.*, 75 (1994) 4000
 27. T. Wagner, R. Molina, T. Yoshinobu, J.P. Klock, M. Biselli, M. Canzoneri, T. Schnitzler and M.J. Schöning, *Electrochim. Acta*, 53 (2007) 305
 28. K. Miyamoto, Y. Kuwabara, S. Kanoh, T. Yoshinobu, T. Wagner and M.J. Schöning, *Sens. Actuators B–Chem.*, 137 (2009) 533
 29. T. Yoshinobu, H. Ecken, A. Poghossian, A. Simonis, H. Iwasaki, H. LuÈth and M.J. Schöning, *Electroanalysis*, 13 (2001) 733
 30. D.E. Yates, S. Levine and T.H. Healy, *J. Chem. Soc., Faraday Trans. 1*, 70 (1974) 1807
 31. M. Nakao, T. Yoshinobu and H. Iwasaki, *Sens. Actuators B–Chem.*, 20 (1994) 119
 32. T. Wagner, C. F.B. Werner, K. Miyamoto, M. J. Schöning and T. Yoshinobu, *Sens Actuators B–Chem.*, 154 (2011) 124
 33. K.-i. Miyamoto, T. Wagner, T. Yoshinobu, S. Kanoh and M. J. Schöning, *Sens. Actuators B–Chem.*, 154 (2011) 28
 34. K.-i. Miyamoto, K. Kaneko, A. Matsuo, T. Wagner, S. Kanoh, M. J. Schöning and T. Yoshinobu, *Sens. Actuators B–Chem.*, 170 (2012) 82